JOURNAL OF CATALYSIS 141, 548–565 (1993)

Isomerization of Xylene and Methylation of Toluene on Zeolite H-ZSM-5. Compound Kinetics and Selectivity

KLAUS BESCHMANN AND LOTHAR RIEKERT[1]

Institut für Chemische Verfahrenstechnik der Universität Karlsruhe, D-7500 Karlsruhe, Germany

Received July 3, 1992; revised February 1, 1993

The alkylation of toluene with methanol and the isomerization of xylene were investigated separately and in detail on zeolite H-ZSM-5 as catalyst. The influence of crystal size alone on rates and product distributions was studied for two Si/Al ratios in the zeolite at 573 and 723 K in a gradientless batch-reactor. The isomer distribution in the xylene resulting from toluene methylation is constant from zero up to at least 50% conversion of the methanol in a stoichiometric mixture, H-ZSM-5 being always *para*-selective. *para*-Xylene prevails increasingly in the products when either crystal size, temperature, or Al content in the zeolite increase; essentially pure *p*-xylene can be obtained in the limit with unmodified H-ZSM-5 as catalyst. The rate of isomerization of xylene alone to an equilibrium mixture of isomers was found to be roughly proportional to the extent of the (external) surface of the zeolite crystals, the ratios of the rates of different reactions in the triangular scheme of isomerization being nearly independent of crystal size. The observations can be understood as resulting from the interaction of reaction and diffusion in the volume of the crystals.

INTRODUCTION

The ample literature on shape-selectivity in zeolite catalysis has been reviewed at intervals by Csicsery (*1*, *2*). Shape-selectivity was first described by Weisz and Frilette (*3*) and explained as a molecular sieve effect leading to a sharp screening of either reactants or products according to molecular size and shape. This concept was then elaborated in experiment and theory by Weisz *et al.* (*4*). A more subtle form of shape-selectivity was described by Chutoranski and Dwyer (*5*), who found that the kinetics of isomerization of xylenes in a zeolite catalyst depends on the size of the crystals and could be represented by a mathematical model assuming different diffusivities of the xylene isomers in the crystals. In this case none of the reactants or products are excluded entirely from entering or leaving the zeolite crystals, but differences in diffusivities of isomers affect kinetics and product composition. Chen and Garwood (*6*) proposed to explain the selectivities observed for various reactions in zeolite H-ZSM-5 not as resulting from sharp molecular sieving but from differences in intracrystalline mobility due to steric hindrance, as did also Chen *et al.* (*7*) when they observed enhanced formation of *para*-xylene in the methylation of toluene on zeolite H-ZSM-5 only in larger crystals or after "modification" of the zeolite with phosphorus. A concise theory of enhanced *para*-xylene selectivity in this system was presented by Wei (*8*) in the form of a mathematical model representing the kinetics of simultaneous intracrystalline alkylation and subsequent isomerization of xylenes, assuming linear kinetics and different diffusivities of xylene isomers in the zeolite crystals. It follows from this theory that a variation of crystal size alone (all other parameters being constant) can influence the product composition of toluene methylation at low conversion. However, when other properties of the zeolite catalyst such as its chemical composition are altered, then a change in product composition is not necessarily due to different conditions of intracrystalline mass transfer, because also the rate coeffi-

[1] To whom correspondence should be addressed.

0021-9517/93 $5.00

cients of intracrystalline reactions will depend on catalyst composition.

The literature concerning the methylation of toluene on zeolite H-ZSM-5 is abundant (*7, 9–24*); the objective of many investigations seems to have been the attainment of high *para*-selectivity through modification of catalyst composition. Isomer composition of product xylene was mostly observed in integral reactors at complete or unknown conversion of one reactant, so that selectivities reported are influenced by secondary isomerization to an unknown extent. In view of the fundamental interest in diffusion mediated shape-selectivity, we have investigated the kinetics and selectivity of methylation of toluene with methanol in zeolites H-ZSM-5 of constant composition but different crystal size and separately the kinetics of xylene isomerization on the same catalysts. A great number of observations was required in order to obtain detailed information of product composition as function of contact time and conversion for different catalysts at several temperatures. The kinetic experiments were therefore conducted in a well mixed closed system (batch-reactor), where product composition can be obtained in one run for a wide range of conversion and contact time through periodic analysis of the gas phase.

EXPERIMENTAL

(*a*) *Zeolites*

Zeolites ZSM-5 were synthesized by crystallization with either tetrapropylammoniumbromide (Si/Al = 160) or *n*-propylamine and triethylamine (Si/Al = 44) as templates without agitation within 4 days under autogenous pressure. Gel composition corresponded to

$$Al_2(SO_4)_3 \cdot k\ SiO_2 \cdot m\ NaOH \cdot n\ H_2O,$$

with k = 88 or 320, m = 7–24, and n = 2000–4000. The molar amount of template added corresponded to about 1 m (in case of Si/Al = 160) or 2 m (Si/Al = 44). Different crystal sizes were obtained by variation of crystallization temperature (433 to 458 K) and of pH. The resulting crystalline materials were shown by XRD to correspond to the MFI-structure with 100% crystallinity. The zeolites were calcined in air at 823 K for 20 h, then exchanged three times with excess 1 *M* NH_4Cl solution at 373 K for 4 h, washed, and dried at 393 K. Through subsequent calcination at 823 K in air for 20 h the ammonium form was converted to the hydrogen from (H-ZSM-5). Composition was determined by wet chemical analysis, crystal size by SEM; characteristic length L is defined as the ratio of volume to (external) surface of the crystals; SEM micrographs are shown in Fig. 1; aluminium distribution was determined by electron microprobe. The results reported in the following were obtained with the zeolites listed in Table 1, which showed no inhomogeneity (zoning) in Al distribution and are of the same shape for a given composition. It was thus possible to compare catalytic properties of zeolites which vary only with respect to crystal size L. It should be noted, however, that it is not possible to prepare strictly monodisperse crystals. The value of the size parameter L has to be understood as an approximate average. The zeolites were pressed into pellets (1900 bar) without binder, the pellets were crushed, a particle size fraction of 0.5 to 1 mm was obtained by sieving and used as catalysts.

(*b*) *Observation of Kinetics*

Reaction kinetics and product distribution were observed in a well mixed batch-reactor system (Fig. 2) containing the zeolite catalyst in contact with a gas phase consisting mainly of nitrogen as inert gas.

TABLE 1
Zeolites

Designation	Si/Al	Crystal size (μm)	L (μm)
S44 (small)	44	9 × 3 × 3	0.64
L44 (large)	44	36 × 10 × 10	2.2
S160 (small)	160	1 μ dia	0.12
L160 (large)	160	2.3 μm dia	0.33

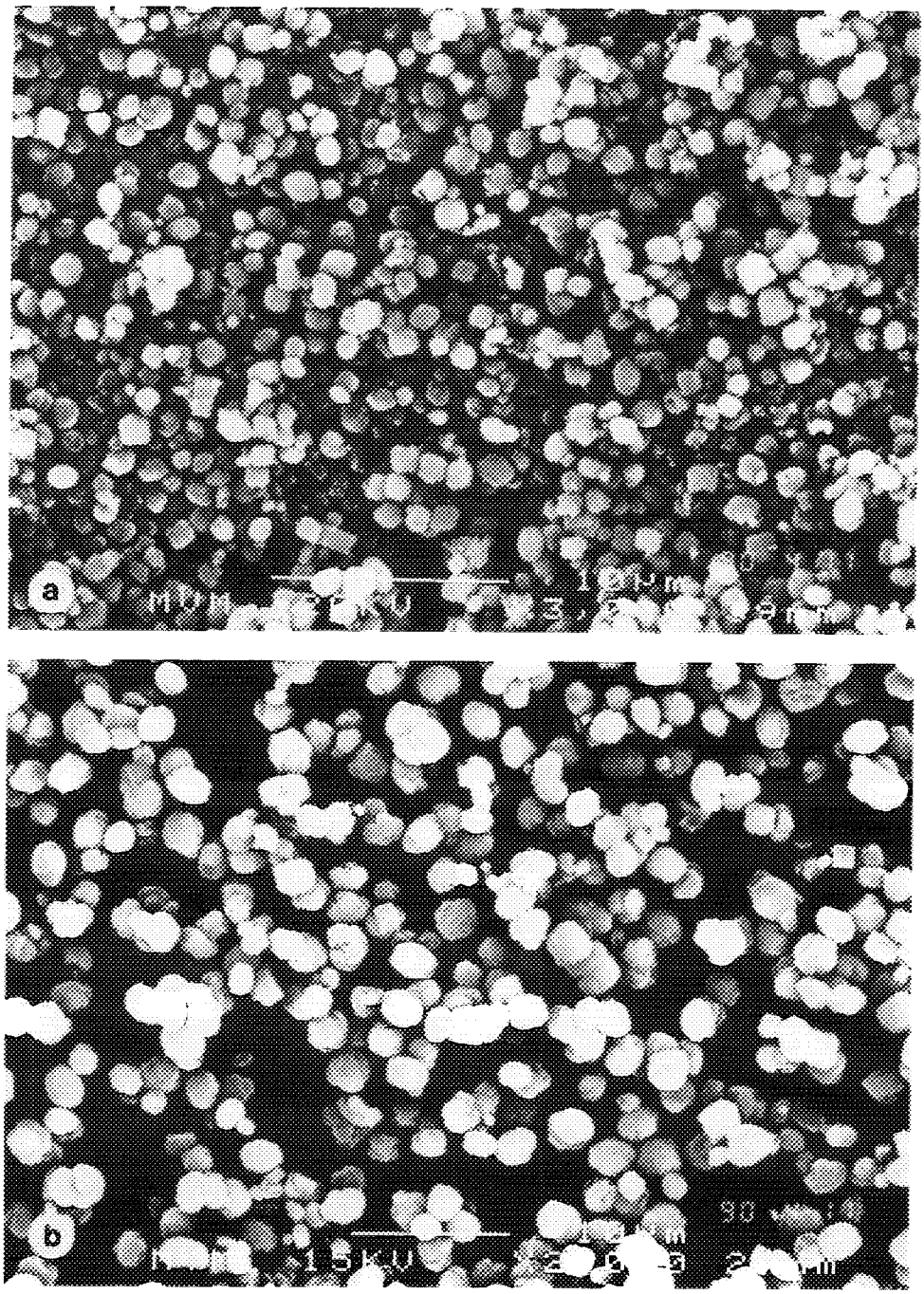

FIG. 1. SEM micrographs of zeolites used as catalysts. (a) S160, (b) L160, (c) S44, and (d) L44.

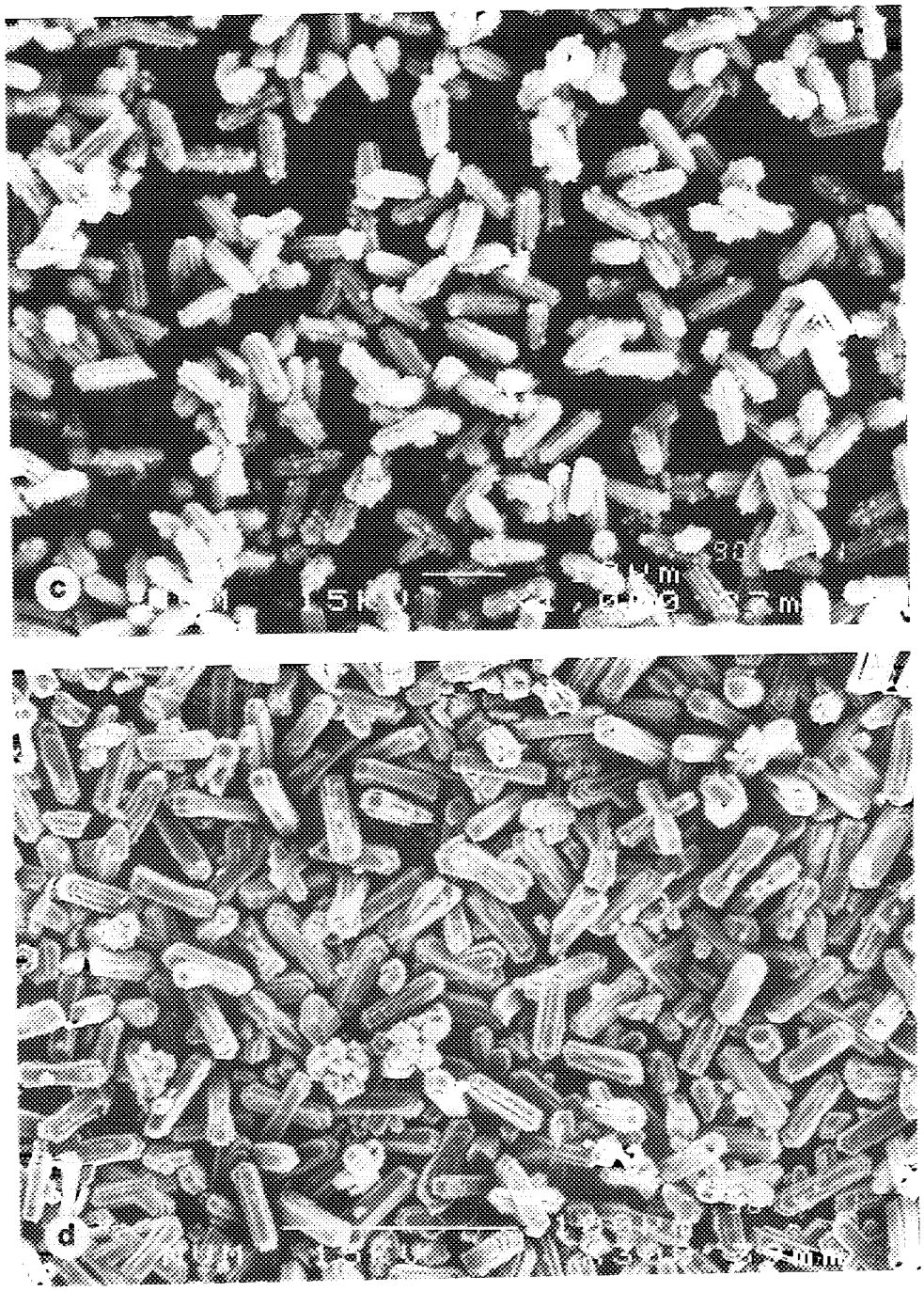

FIG. 1—*Continued*

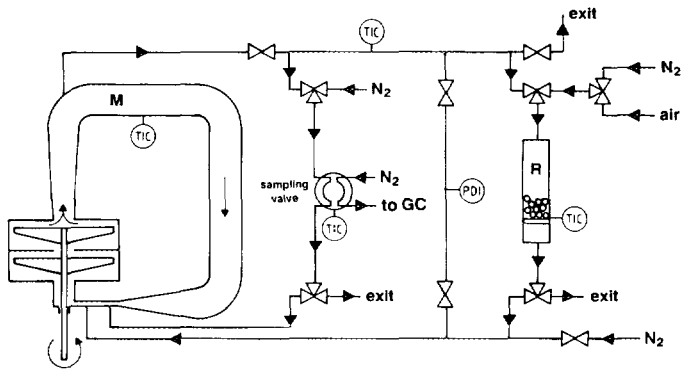

FIG. 2. Gradientless batch reactor system, schematic. M: mixing loop and radial blower (at 433 K); R: quartz reactor at temperature T.

To start an experiment liquid reactants (37 to 789 μl) are injected with a syringe through a Teflon-backed septum at $t = 0$ and the composition of the gas phase is then analyzed periodically through capillary gas chromatography. The gas is circulated at a rate of more than 2 liter/s through a mixing loop M of 6.6 liter volume by means of a radial blower with a two-stage rotator (14,000 rpm). The pressure difference of 65 mbar in the mixing loop is sufficient to drive a flux of 0.13 liter/s through the reactor loop R containing the catalyst in a quartz reactor heated to reactor temperature T, and through the gas sampling valve, which is held at 503 K. The reactor operates in the differential mode, so that the entire system can be considered as well mixed. The mixing loop M as well as all connecting lines are made of stainless steel and are heated to 433 K to prevent condensation of reactants or products. The principle of the experimental method has been described previously (*25*); details of the improved version of the apparatus used in the present work are described in Ref. (*26*).

The procedure in the experiments was as follows: the zeolite catalyst (between 20 and 500 mg) is placed on the quartz frit in the reactor and heated to 823 K in nitrogen (99.999%) for 12 h, the reactor being disconnected from the mixing loop M, which is evacuated and filled with nitrogen to a pressure of 20 mbar above ambient. The catalyst is then brought to reactor temperature T and the reactants are introduced into the mixing loop M. Their partial pressures are obtained from the amounts injected and verified by reading the pressure increase following the injection through a capacitance manometer. Hydrocarbons *p*-, *m*-, and *o*-xylene and toluene were obtained from Fluka Chemie as puriss. grade; methanol p.a. 99.8% from Merck AG. A sample of the mixture in M is analyzed by GC and the reactor is then connected at $t = 0$ with volume M; thereafter the composition of the gas phase is analyzed periodically, two sample loops (0.5 cm^3 each) being used alternately. An experimental run lasts between 3 and 8 h. Afterwards the reactor is disconnected and the catalyst is heated to 823 K in a stream of dry air for 12 h to burn any carbonaceous deposits before another run is started; the initial activity is always regained through treatment with air at 823 K. The mixing volume M is flushed with nitrogen until no hydrocarbon can be detected. From the gas-chromatographic analysis one obtains the partial pressure p_i of component i relative to the initial partial pressure $p_{A,0}$ of reactant A in the closed system as a function of time:

$$\frac{p_i\{t\}}{p_{A,0}} = f_{i,A}\{t\}. \qquad (1)$$

The conversion X_A of reactant A is then

$$X_A = 1 - f_{A,A}, \tag{2}$$

and the mass-specific rate of reaction of reactant A (m = mass of catalyst) is

$$(r_m)_A \equiv -\frac{1}{m}\cdot\frac{dn_A}{dt} = \frac{dX_A}{d(tm)}\cdot n_{A,0} = \frac{dX_A}{d(tm)}\cdot\frac{p_{A,0}}{\text{mbar}}\cdot 1.83\times 10^{-4}\ \text{mol}, \tag{3}$$

where $n_{A,0}$ has been expressed through the ideal gas law with $V = 6600\ \text{cm}^3$, $T = 433$ K, the volume of the quartz reactor being negligible compared to that of the thermostated mixing loop M.

Results obtained with different amounts of catalyst can be represented on the common timescale $t \cdot m$. The yield y_i of product i relative to the initial amount $n_{A,0}$ of reactant A is

$$y_i = \frac{n_i}{n_{A,0}} = f_{i,A}, \tag{4}$$

and for the mass-specific rate of production of i we have

$$r_m^i \equiv \frac{1}{m}\cdot\frac{dn_i}{dt} = \frac{dy_{i,A}}{d(tm)}\cdot\frac{p_{A,0}}{\text{mbar}}\cdot 1.83\times 10^{-4}\ \text{mol}. \tag{5}$$

The isomer composition of xylene is described in the following by the ratio x_i of the amount n_i of isomer i ($i = o$, m, or p) to the total amount of xylene in the gas phase:

$$x_i \equiv \frac{n_i}{n_o + n_m + n_p} = \frac{f_i}{f_o + f_m + f_p}. \tag{6}$$

RESULTS

(a) *Isomerization of Xylene*

The evolution of the distribution of xylene isomers with time in the closed system is shown in Fig. 3 for a catalyst temperature of 723 K and two zeolites with the same Si/Al-ratio of 44 but different crystal size. Observations on catalysts with Si/Al = 160 and different crystal size are represented in Fig. 4 as reaction paths in triangular coordinates, where observations with the same catalyst but different initial compositions are also shown. All reaction paths led to an equilibrium distribution x_i^* agreeing with values calculated from thermodynamic data (*27*):

T (K)	$(x_p^*)_{obs}$	$(x_p^*)_{calc}$	$(x_m^*)_{obs}$	$(x_m^*)_{calc}$
573	.24	.243	.54	.541
723	.23	.236	.53	.525

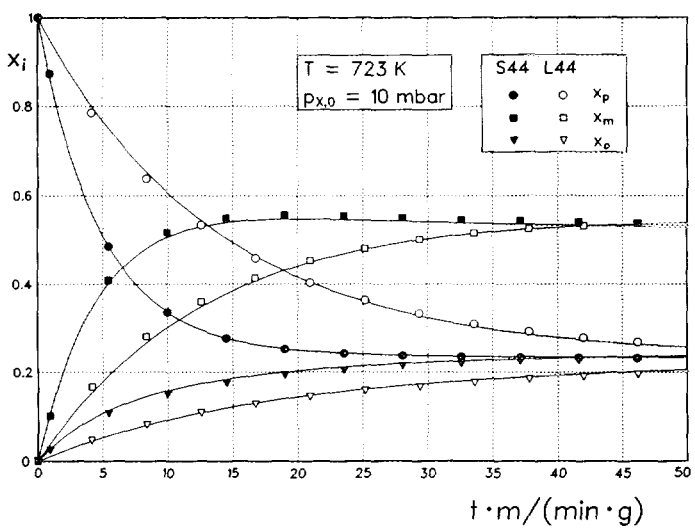

FIG. 3. Isomerization of *para*-xylene to equilibrium mixture on catalysts S44 and L44 at 723 K; mole fractions x_i of different isomers as function of modified time $t \cdot m$; $p_X = 10$ mbar.

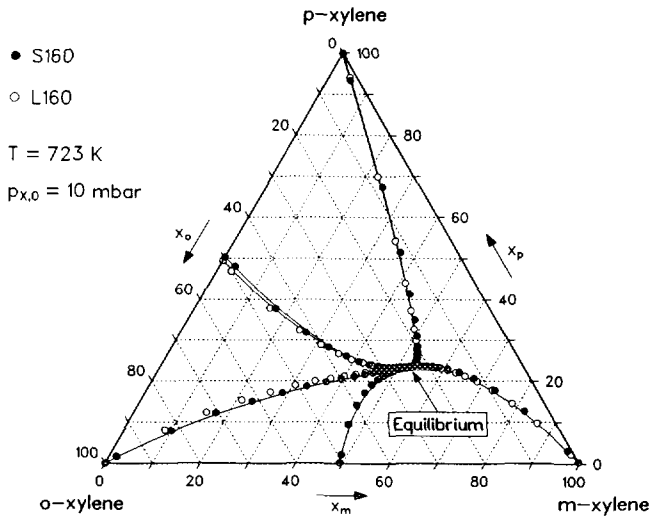

FIG. 4. Reaction paths in triangular coordinates representing mole fractions of xylene isomers. Catalysts S160 (●) and L160 (○); T = 723 K; p_X = 10 mbar.

The rate of conversion towards equilibrium depends on crystal size (Fig. 3), whereas the composition of the ternary system moves from a given initial point to equilibrium along a path which depends mainly on temperature and zeolite composition (Si/Al ratio). For five initial compositions (pure isomers and mixtures $o + p$ and $o + m$ in 1 : 1 ratio, partial pressure of xylene 10 mbar) the kinetics of isomerization was observed at 573 and 723 K on all four zeolites and found to be reproducible within experimental accuracy (±3% in x_i). The detailed data are listed and graphs of the resulting 40 reaction paths are shown in Ref. (*26*). At 723 K all reaction paths were found to be independent of crystal size within the limits of experimental error. At the lower temperature of 573 K a slight dependence of the reaction paths on crystal size was reproducibly noticeable, as shown in Fig. 5 for zeolites S160 and L160.

Side reactions such as disproportionation of xylene to benzene and trimethylbenzene were insignificant, involving less than 10% of the initial amount of xylene. The kinetics of xylene isomerization can be represented as a triangular network of reactions which are first order in the concentrations of the respective isomers in the gas phase:

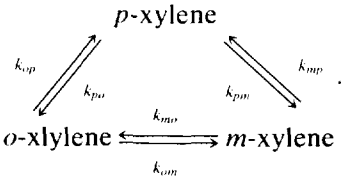

Following Wei (*8*), the system of simultaneous rate equations can be written in matrix form

$$\frac{1}{m}\begin{pmatrix}\dot{n}_p\\ \dot{n}_m\\ \dot{n}_o\end{pmatrix} = \begin{pmatrix}-(k_{pm} + k_{po}) & k_{mp} & k_{op}\\ k_{pm} & -(k_{mp} + k_{mo}) & k_{om}\\ k_{po} & k_{mo} & -(k_{op} + k_{om})\end{pmatrix}\begin{pmatrix}c_p\\ c_m\\ c_o\end{pmatrix} \qquad (7)$$

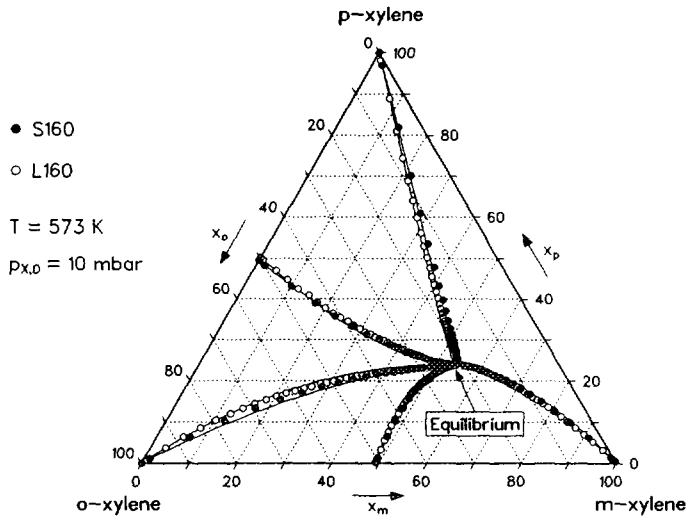

FIG. 5. Reaction paths on catalysts S160 (●) and L160 (○) at 573 K, p_X = 10 mbar.

or

$$\frac{\vec{n}}{m} = k_{pm} \cdot \mathbf{K} \cdot \vec{c} \qquad (8)$$

where $\vec{n}$: column vector of rates $\dot{n}_i$ in mol · s^{-1} (n_i = amount of gaseous isomer i).

$\vec{c}$: column vector of gas-phase concentrations c_i of xylene isomers in mol · cm^{-3}.

k_{pm}: rate constant k_{pm} in $cm^3\ g^{-1}\ s^{-1}$.

K: matrix of dimensionless rate coefficients k'_{ij} with $k'_{ij} \equiv k_{ij}/k_{pm}$.

The reaction path in the triangular simplex depends only on the dimensionless matrix **K**, which determines the ratios of the rates of individual reactions in the triangular scheme, observed as a change of gas phase composition.

First-order rate coefficients k_{ij} were obtained by computerized multiple linear regression from the observed dependence of $\vec{c}$ on $t \cdot m$. They are listed in Table 2 as defined in Eqs. (7) and (8) and they represent the observations correctly as shown by the solid lines in Figs. 3, 4, and 5 (the effect of deactivation during one run being ne-

TABLE 2

Kinetic Coefficients of Xylene Isomerization

Zeolite	T (K)	k_{pm} ($cm^3\ g^{-1}\ s^{-1}$)	**K**
S160	573	2.40	$\begin{pmatrix} -1.40 & .44 & .43 \\ 1.00 & -.65 & .50 \\ .40 & .21 & -.93 \end{pmatrix}$
L160	573	1.51	$\begin{pmatrix} -1.45 & .44 & .48 \\ 1.00 & -.60 & .38 \\ .45 & .16 & -.86 \end{pmatrix}$
S160	723	16.2	$\begin{pmatrix} -1.31 & .44 & .30 \\ 1.00 & -.60 & .35 \\ .31 & .16 & -.65 \end{pmatrix}$
L160	723	7.36	
S44	573	8.82	$\begin{pmatrix} -1.30 & .44 & .32 \\ 1.00 & -.51 & .18 \\ .30 & .073 & -.50 \end{pmatrix}$
L44	573	2.02	$\begin{pmatrix} -1.36 & .44 & .39 \\ 1.00 & -.54 & .25 \\ .36 & .10 & -.64 \end{pmatrix}$
S44	723	23.2	$\begin{pmatrix} -1.27 & .44 & .26 \\ 1.00 & -.51 & .16 \\ .27 & .074 & -.42 \end{pmatrix}$
L44	723	7.91	

glectable), which have been calculated from the data in Table 2. For a given Si/Al ratio in the zeolite and $T = 723$ K only one matrix **K** for small and large crystals is listed in Table 2, since the reaction paths in the triangular simplex did not depend on crystal size at 723 K within experimental accuracy. The entries in the matrix **K** should be considered as reliable within ±5%, although **K** was obtained from observations with five widely different initial compositions in each case. Whereas the reaction path for a given Si/Al ratio appears to be almost independent of crystal size, the rate of approach to equilibrium is strongly dependent on crystal size as shown by the values of the scalar factor k_{pm} in Table 2.

(b) Methylation of Toluene

Conversion X_M of methanol and the cumulative yield y_X of xylenes on zeolites S160 and L160 at 573 K are shown as function of modified time $m \cdot t$ in Fig. 6, the isomer distribution in the product xylene as function of methanol conversion in Fig. 7. Results obtained at different temperatures (573 and 723 K) for all four zeolites followed the same pattern, illustrated in Figs. 6 and 7 as an example. This pattern can essentially be summarized as follows.

(1) Conversion of methanol is much faster than conversion of toluene, so that even with a 2 : 1 excess of methanol in the reactants less than 30% of toluene has been converted to xylene when only 5% of the methanol is left. Methanol disappears mainly by reacting to aliphatic hydrocarbons (MTG-process), as has been pointed out by Chen (*20*).

(2) The isomer distribution in the product xylene is essentially constant up to a conversion of methanol of 50%, with all three isomers generated simultaneously, the ratios of their respective rates of formation (isomer selectivity) being constant as long as the partial pressure of reactant methanol is sufficient. The isomer distribution approaches equilibrium when the methanol has been nearly consumed ($X_M > 0.8$).

(3) Toluene is also alkylated to trimethylbenzene and disproportionates. However, less than 20% of the toluene converted disappears in these or other side-reactions.

In order to quantify the observations with different catalysts under different condi-

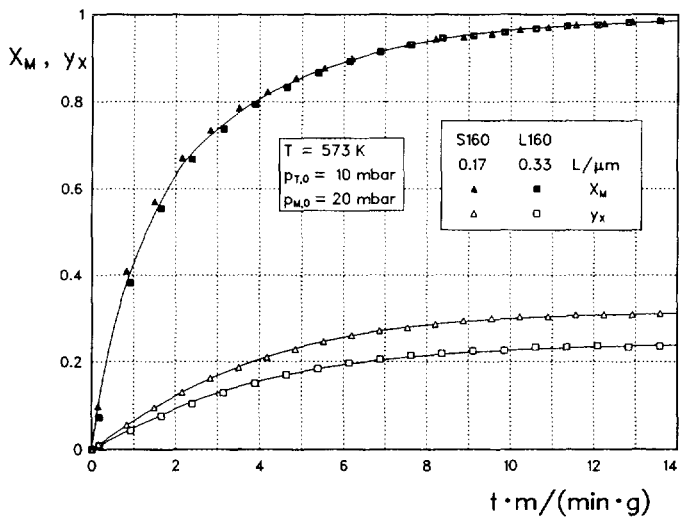

FIG. 6. Conversion X_M of methanol (▲, □) and yield y of xylene (△, □) on catalysts S160 (▲, △) and L160 (■, □) as function of modified time $t \cdot m$ at 573 K; $p_{M,0} = 20$ mbar, $p_{T,0} = 10$ mbar.

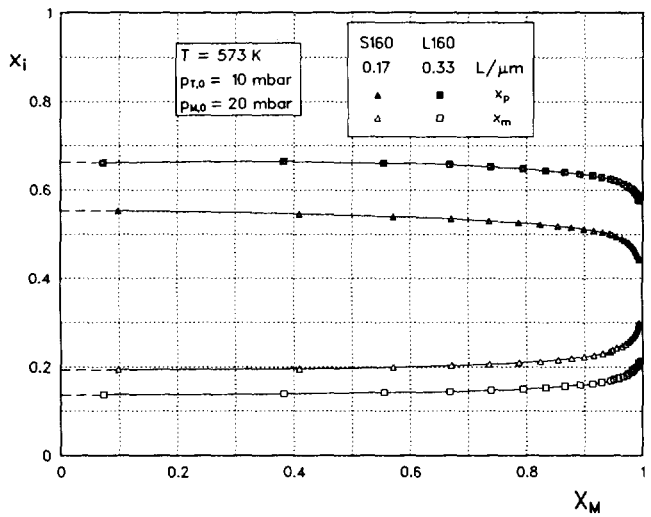

FIG. 7. Mole fraction x_p (▲, ■) and x_m (△, □) of *para*- and *meta*-xylene in product xylene as function of conversion X_M of methanol. Catalysts S160 (▲, △) and L160 (■, □): T = 573 K; $p_{M,0}$ = 20 mbar, $p_{T,0}$ = 10 mbar. $x_o = 1 - (x_p + x_m)$.

TABLE 3

Rate and Selectivity of Reaction of Toluene with Methanol

Catalyst	T (K)	$p_{T,0}$ (mbar)	$p_{M,0}$ (mbar)	$(r_m^M)_0$ (mol g^{-1} s^{-1})	$(r_m^X)_0$ (mol g^{-1} s^{-1})	$(x_p, x_m, x_o)_{X_M<0.5} \equiv \vec{x}_0$		
S160	573	10	5	1.2×10^{-5}	1.2×10^{-6}	.54	.20	.26
		10	10	2.3×10^{-5}	1.9×10^{-6}	.55	.19	.26
		10	20	3.9×10^{-5}	2.1×10^{-6}	.55	.19	.26
		20	20	3.8×10^{-5}	2.1×10^{-6}	.51	.20	.28
		40	20	3.7×10^{-5}	3.5×10^{-6}	.51	.20	.29
L160	573	10	5	0.8×10^{-5}	0.9×10^{-6}	.64	.15	.21
		10	10	1.5×10^{-5}	1.0×10^{-6}	.64	.15	.21
		10	20	2.6×10^{-5}	1.4×10^{-6}	.66	.14	.20
		20	20	4.2×10^{-5}	2.7×10^{-6}	.66	.15	.19
		40	20	3.6×10^{-5}	3.6×10^{-6}	.66	.14	.20
	723	20	20	9.4×10^{-5}	1.4×10^{-5}	.84	.09	.07
		20	40	1.9×10^{-4}	1.8×10^{-5}	.85	.08	.07
S44	573	10	5	3.4×10^{-5}	3.9×10^{-6}	.91	.05	.04
		10	10	6.1×10^{-5}	4.1×10^{-6}	.92	.04	.04
		10	20	1.1×10^{-4}	4.5×10^{-6}	.92	.05	.03
L44	573	10	5	2.5×10^{-5}	1.9×10^{-6}	.92	.04	.04
		10	10	3.5×10^{-5}	2.0×10^{-6}	.92	.04	.04
		10	20	7.9×10^{-5}	1.9×10^{-6}	.92	.04	.04
		20	20	8.1×10^{-5}	5.5×10^{-6}	.93	.04	.03
		20	40	1.4×10^{-4}	5.8×10^{-6}	.92	.04	.04
	723	20	20	2.0×10^{-4}	2.5×10^{-5}	.95	.03	.02
		20	40	3.9×10^{-4}	3.0×10^{-5}	.95	.03	.02

tions the following data are listed in Table 3:
—initial mass specific rates of conversion of methanol $(r_m^M)_0$ and of formation of xylene $(r_m^X)_0$ in mol g^{-1} s^{-1};
—isomer distribution (selectivity) in the range $0 < X_M < 0.5$.
For a given zeolite the rate of conversion of methanol appears to be proportional to its partial pressure; the rate of formation of xylene increases with p_M as well as with p_T, but less strongly than proportionality would require. At 573 K methanol conversion on catalyst S44 is faster than on L160 under otherwise identical conditions by a factor of 4.2 ± 0.1; for xylene formation the ratio is 3.7 ± 0.6, whereas the ratio of Al-content is 160:44 = 3.6. A dependence of the observed rates of reaction on crystal size beyond the scatter of the data is clearly discernible only if the rates observed for the more active catalysts with Si/Al = 44 but different size (S44 versus L44) are compared: at 573 K the average ratio of rates under otherwise identical conditions is 1.5 ± 0.2 for methanol conversion and 2.2 ± 0.2 for xylene formation, whereas the inverse of the ratio of characteristic lengths is 2.2:0.64 = 3.4. Much more pronounced is the influence of crystal size on the isomer distribution of the product xylene. *para*-Selectivity increases conspicuously with crystal size, as shown by the data for zeolites S160 and L160 in the last column of Table 3. It also increases with temperature and mass-specific activity (Al-content) of the zeolite, which means with the mass-specific rate constant of xylene formation. The de-

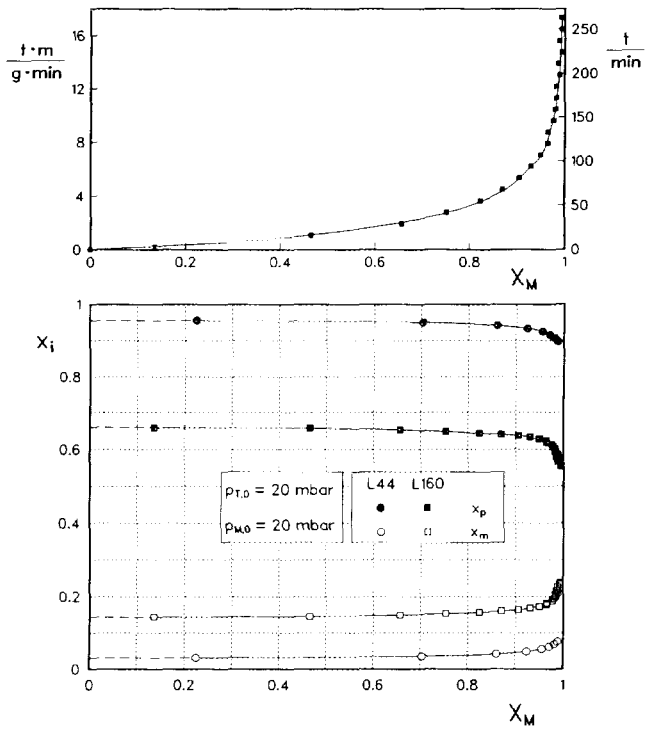

FIG. 8. Mole fraction x_p (●, ■) and x_m (○, □) of *para*- and *meta*-isomers in product xylene as function of conversion X_M of methanol. $x_o = 1 - (x_p + x_m)$: (●, ○) catalyst L44, $T = 723$ K, $p_{T,0} = p_{M,0} = 20$ mbar; (■, □) catalyst L160, $T = 573$ K, $p_{T,0} = p_{M,0} = 20$ mbar. Clock time t and modified time $t \cdot m$ as function of the independent variable X_M are shown in the upper part of the diagram for observations on catalyst L160.

pendence of para-selectivity on crystal size is thus less pronounced with the more active zeolites S44 and L44, where it exceeds already 90% on the smaller crystals.

All four zeolites were found to be para-selective in the sense that the content of *para*-isomer in the xylene generated exceeded by far the equilibrium value as long as enough methanol was present to sustain xylene formation. Integral and differential isomer selectivity then coincide practically and correspond to initial selectivity as shown in Fig. 8 for zeolites with Si/Al of 160 and 44. It may be noted that this characteristic feature of methylation of toluene on zeolite ZSM-5 cannot be observed if product composition is observed only at the exit of an integral reactor at full conversion of methanol.

DISCUSSION

From the experimental observations reported here, two conclusions can be drawn which appear essential concerning the influence of intracrystalline mass transfer on rates and product distribution in alkylation of toluene and concomitant isomerization of xylene. These are as follows:

(1) The isomer distribution of xylenes, resulting from the reaction of toluene with methanol is constant from zero up to at least 50% conversion of methanol starting from a stoichiometric mixture; it depends on the size of the crystals for a given Si/Al ratio. The *para*-isomer prevails in the products increasingly when crystal size, temperature and/or Al content increase, so that essentially pure *p*-xylene can be obtained in the limit with unmodified H-ZSM-5 as catalyst.

(2) The reaction paths observed for the isomerization of xylene to an equilibrium mixture are independent of crystal size at 723 K and depend only slightly on crystal size at 573 K. The ratio of the mass-specific rate coefficients k_{pm} (Table 2) for given Si/Al ratio and temperature corresponds roughly to the ratio of surface/mass (proportional to $1/L$, Table 1). The rate of isomerization is thus found to be approximately proportional to the extent of the surface of the crystals.

The dependence of product distribution on crystal size alone leads immediately to the conclusion that selective intracrystalline mass transfer (of products or some intermediates) has an effect on selectivity. The size of the zeolite crystals cannot have an influence on rate coefficients pertaining to any differential element of volume or surface, but only on the kinetics of mass transfer.

The gaseous products of toluene methylation will undergo isomerization to an equilibrium mixture of xylene isomers in a secondary reaction, because zeolite H-ZSM-5 is a catalyst for alkylation and for isomerization. The rate of secondary isomerization appears to be much smaller than the rate of xylene production from toluene and methanol, unless the latter almost ceases due to exhaustion of reactant methanol (Fig. 8). This conclusion also results from a comparison of the observed rate of *para*-xylene production observed during alkylation, $(dn_p/d(t \cdot m))_{alk}$, with the rate of secondary isomerization of *para*-xylene

$$\left(\frac{dn_p}{d(tm)}\right)_{iso} = -(k_{pm} + k_{po})c_p + k_{mp}c_m + k_{op}c_o \quad (9)$$

evaluated with rate coefficients k_{ij} obtained independently for the same catalyst (Table 2). For zeolite S160 at 573 K and $p_{T,0} = 10$ mbar, $p_{M,0} = 20$ mbar we obtain for different degrees X_M of conversion of methanol the values listed in Table 4. By subtracting the rate of the simultaneously occurring isomerization of *para*-xylene from the observed rate of formation of *para*-xylene a corrected value of *para*-xylene formation from methylation of toluene is obtained, which is listed in the last line of Table 4. The rate of isomerization is less than 10% of the net rate of production observed during toluene alkylation up to $X_M \approx 0.8$; the corrected rate of production of *para*-xylene due to alkylation alone remains constant up

TABLE 4

Rates of *para*-Xylene Formation on Zeolite S160 at 573 K. Net Rates Observed and Rates of Isomerization at Different Degrees of Methanol Conversion

X_M	0.1	0.2	0.3	0.4	0.5	0.6	0.7	0.8	0.9
$\left(\frac{dn_p}{d(t \cdot m)}\right)_{alk}^{obs}$ (mol · g^{-1} · s^{-1})	1.2×10^{-6}	1.2×10^{-6}	1.1×10^{-6}	1.0×10^{-6}	9.5×10^{-7}	8.5×10^{-7}	7.0×10^{-7}	5.0×10^{-7}	2.4×10^{-7}
$\left(\frac{dn_p}{d(t \cdot m)}\right)_{isom}$ (mol · g^{-1} · s^{-1})	-3.3×10^{-9}	-6.9×10^{-9}	-1.1×10^{-8}	-1.6×10^{-8}	-2.2×10^{-8}	-2.9×10^{-8}	-3.9×10^{-8}	-5.2×10^{-8}	-6.6×10^{-8}
$\left(\frac{dn_p}{d(t \cdot m)}\right)_{alk}^{corr}$ (mol · g^{-1} · s^{-1})	1.2×10^{-6}	1.2×10^{-6}	1.1×10^{-6}	1.0×10^{-6}	9.7×10^{-7}	8.8×10^{-7}	7.4×10^{-7}	5.5×10^{-7}	3.1×10^{-7}

to $X_M \approx 0.4$. The isomer distribution observed in toluene alkylation over an extended range of methanol conversion corresponds to the distribution in the limit of zero conversion.

Whereas the isomer distribution (selectivity) of toluene alkylation depends on crystal size, the reverse appears to be true for the isomerization of xylenes on the same catalysts, where reaction paths were found to depend but slightly on crystal size and only at the lower temperature of 573 K. These observations can be understood as a consequence of coupled reaction and diffusion in the zeolite crystals, according to the theory expounded by Wei (*8*). In the case of alkylation as well as in isomerization the matrices of rate coefficients and the product composition which are effectively observable should depend on the same set of generalized Thiele numbers, but in ways that are different for alkylation and isomerization. Assuming that the diffusivity of *para*-xylene is much higher than that of the *ortho*- and *meta*-isomers, the alkylation of toluene alone should yield pure *para*-xylene in the limit of very large crystals, whereas the reaction paths for isomerization of xylenes should for sufficiently large crystals be independent of crystal size, corresponding to a constant matrix of relative rate coefficients.

In order to visualize how this result follows from theory let us consider the simpler (hypothetical) case of only two isomers (e.g., *para* and *ortho*), which are generated in a zeolite crystal (slab of thickness $2L$; one-dimensional geometry) by alkylation in unknown relative proportions x_p' and $x_o' = 1 - x_p'$. In the zeolite they can also isomerize according to

$$o \underset{k_-}{\overset{k_+}{\rightleftharpoons}} p.$$

From the local material balances at steady state

$$\frac{\partial c_p}{\partial t} = r_{al} \cdot x_p' + k_+ c_o - k_- c_p + D_p \cdot \frac{\partial^2 c_p}{\partial x^2} = 0 \quad (10a)$$

$$\frac{\partial c_o}{\partial t} = r_{al}(1 - x_p') + k_- c_p - k_+ c_o + D_o \cdot \frac{\partial^2 c_o}{\partial x^2} = 0 \quad (10b)$$

we have

$$r_{al} + D_p \cdot \frac{d^2 c_p}{dx^2} + D_o \cdot \frac{d^2 c_o}{dx^2} = 0, \quad (11)$$

where x is the distance from the center plane and r_{al} the rate of alkylation per unit of volume. Taking r_{al} to be constant over x (as seems to hold approximately for the zeolites with Si/Al = 160), integration of Eq. (11) yields

$$-\left(D_p \frac{dc_p}{dx} + D_o \frac{dc_o}{dx}\right) = r_{al} \cdot x = \dot{n}', \quad (12)$$

which simply means that the total flux $\dot{n}'$ of xylenes per unit of area through a plane at x equals the rate of production in the volume enclosed by this plane. The concentration profiles for c_p and c_o resulting under the assumption $D_p \gg D_o$ are shown *schematically* in Fig. 9 for boundary condition $c_p = c_o = 0$ at $x = L$, that is, for zero conversion of reactants. The *p*-isomer is continuously withdrawn from the alkylation and from the reversible isomerization in the interior of the crystal, leaving towards the gas phase.

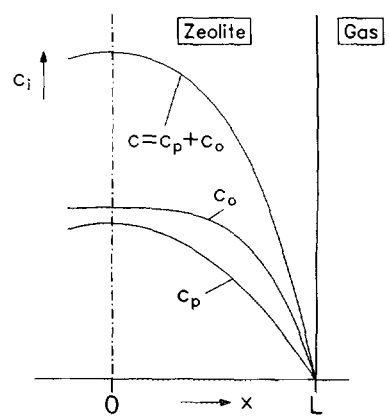

FIG. 9. Concentration profiles (schematic) in flat plate for alkylation leading to two isomers of different mobility. x = distance from center plane, zero conversion of reactants.

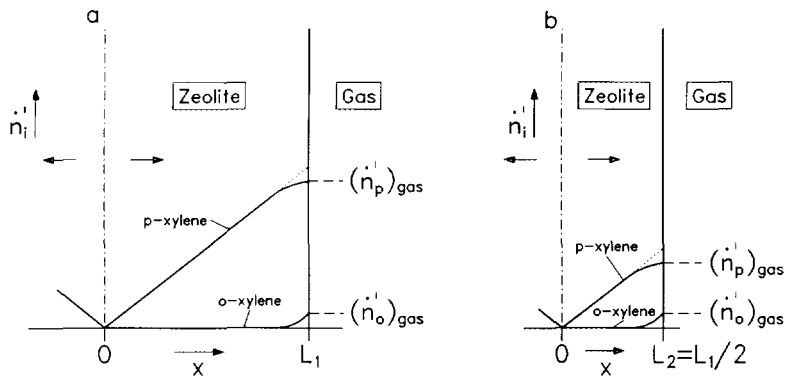

FIG. 10. Fluxes $\dot{n}_i'$ per unit area in flat plates of half thickness L_1 and $L_2 = L_1/2$ for alkylation producing two isomers of different mobility (schematic).

The *o*-isomer does not contribute to the total flux due to its relatively small mobility, except in a region near the surface, where its concentration gradient would otherwise become negative infinite, i.e., the *o*-xylene which is formed by alkylation in the interior of the crystal is isomerized there to *para*-xylene, leaving towards the gas phase from the interior as *para*-xylene. The pattern of corresponding fluxes of both isomers is shown schematically in Fig. 10 for two values of crystal size. The flux of the less mobile *o*-isomer into the gas phase is not affected by the size parameter L, whereas the flux of the *p*-isomer at $x = L$ increases with L. Essentially pure *p*-isomer will be obtained as gaseous product in the limit when crystal size L increases. The total flux $\dot{n}'$ at $x = L$ and concomitantly the mole fraction of the *p*-isomer in the gaseous product should also increase with temperature and/or Al content of the zeolite, as has been observed. The irreversible alkylation of toluene is an internal source of xylene isomers in the zeolite, which is the driving force imposing the concentration profiles depicted schematically in Fig. 9. In the case of isomerization of xylene from the gas phase this driving force is absent and we have from Eq. (12) with $r_{al} = 0$

$$D_p \cdot \frac{dc_p}{dx} + D_o \cdot \frac{dc_o}{dx} = 0. \qquad (13)$$

For a gas phase not in isomer equilibrium consisting of pure *p*-isomer a concentration distribution as shown schematically in Fig. 11 can be expected in the crystal. Here the isomers will be in mutual equilibrium in the interior of the crystal, net isomerization reaction being restricted to a region near the surface. The fluxes of either isomer are coupled according to Eq. (13); diffusivity of the less mobile isomer together with the intracrystalline rate coefficients of isomerization determines the restricted depth δ of penetration of the reaction. For $L > \delta$ the rate of isomerization will become propor-

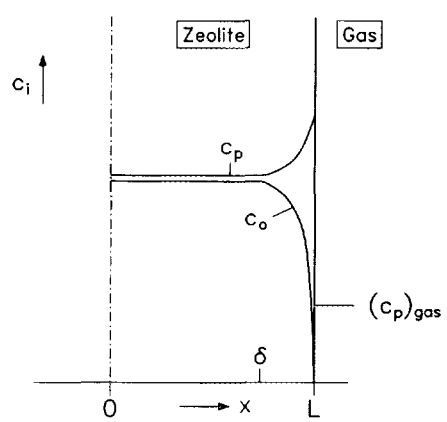

FIG. 11. Concentration profiles (schematic) in flat plate for isomerization, intracrystalline equilibrium condition $(x_p/x_o)^*_{intra} = k_+/k = 1$ assumed.

tional to the extent of surface of the zeolite crystals and the reaction path in the case of more than one relatively immobile isomer will then be independent of crystal size L.

Wei's theory of enhanced para-selectivity stipulates in essence that the relatively immobile *ortho*- and *meta*-isomers emanating into the gas phase are generated within a restricted depth δ of penetration into the zeolite, the interior volume of the crystal being a source of the more mobile *para*-isomer in the case of alkylation. All experimental observations reported here can be understood on the basis of this theory if one assumes that the thickness δ of the layer exchanging the less mobile *ortho*- and *meta*-xylenes with the gas phase is smaller than the characteristic length L of the larger crystals for each Si/Al ratio.

An alternative explanation of the observed selectivity patterns can be based on the assumption that the volume of the zeolite crystal and its surface are different loci of catalytic activity with distinct properties, *meta*- and *ortho*-xylene being generated or reacting only on the surface. Isomerization would in this case be restricted to the surface, alkylation would occur on the surface and in the volume, the volume contributing only *para*-xylene to the products, so that the latter preponderates with increasing volume/surface ratio. This explanation of observed selectivity as due to sharp molecular screening has been proposed by Fraenkel and co-workers (*13, 23*) and also by Nunan *et al.* (*28*). It can be considered as an extreme case within the theory expounded by Wei (*8*), the thickness δ of the surface-near region exchanging all three isomers with the gas phase being then zero. The conclusion $\delta < L$ resulting from our observations includes the extreme case $\delta = 0$ as a possibility.

A stringent discrimination between either coupling of reaction and diffusion in the zeolite crystal on the one hand, or sharp molecular screening on the other hand as the adequate concept explaining product shape-selectivity would require evaluation of the concentration profiles in the crystal from experimental data. For this purpose one needs as an input besides rate of reaction and selectivity also the intracrystalline diffusion coefficients of all three xylene isomers and their equilibrium distribution in the crystal under reaction conditions. These data are not available. From sorption kinetics it can be concluded that the mobility of *para*-xylene in ZSM-5 is much greater than that of *ortho*-xylene; however it was not possible to obtain a diffusivity for transient uptake of the *ortho*-isomer (*29, 30*). A ratio $D_p/D_o \approx 10^3$ has been quoted repeatedly in the literature (e.g. (*8, 13, 31*)), but it is not clear how it has been observed. Moreover, the diffusivities under conditions of reaction depend on the mobilities and concentrations of all compounds in the zeolite, including reactants; the rates of mass transfer will thus be interdependent, as has been shown by Qureshi and Wei (*32*). Reliable equilibrium sorption isotherms have not been obtained for *ortho*- and *meta*-xylene in ZSM-5; the intracrystalline equilibrium constants cannot therefore be deduced from the data valid for the gas phase. The question to what extent *ortho*- and *meta*-xylene react or are generated in the volume and on the surface of the zeolite crystals, respectively, cannot therefore be answered rigorously in a quantitative way on the basis of existing knowledge. However, isomerization of xylene and production of the *meta*- and *ortho*-isomers cannot be entirely restricted to the crystal surface, because not only *para*- but also *meta*- and *ortho*-xylene are sorbed in the volume of ZSM-5 (*20, 29, 30, 33*), their intracrystalline diffusivity being different from zero, as has been specifically demonstrated by Chen (*20*). Mirth and Lercher (*34*) observed by IR-spectroscopy that the concentrations of *m*- and *o*-xylene exceed that of *p*-xylene in the volume of ZSM-5 during methylation of toluene. The slight but reproducible dependence of the reaction paths of xylene-isomerization on crystal size at 573 K indicates that the reactions

involve an exchange also of the less mobile isomers between the volume of the crystal and the gas phase.

ACKNOWLEDGMENTS

We are indebted to J. Zhou for preparing the zeolites used in this study and to U. Müller at BASF Ludwigshafen for determining Al distribution in the crystals. This work was supported by the Deutsche Forschungsgemeinschaft as a project in Sonderforschungsbereich 250.

APPENDIX: NOTATION

Variables

c	Amount concentration (mol · m^{-3})
$f_{i,A}$	Ratio of partial pressure of component i relative to the initial partial pressure of reactant A (—)
k_{ij}	Mass-specific rate constant (cm^3 g^{-1} s^{-1})
k	Volume-specific rate constant (s^{-1})
m	Mass of catalyst (g)
n	Amount of substance (mol)
$\dot{n}$	Amount flow rate (mol · s^{-1})
$\dot{n}'$	Amount flow rate per unit area (mol · m^{-2} s^{-1})
p	Pressure (bar)
r_m	Mass-specific rate of reaction or production (mol · g^{-1} s^{-1})
r_{al}	Volume-specific rate of alkylation (mol · cm^{-3} s^{-1})
t	Clock time (s)
x	Coordinate (m)
x_i	Fraction of isomer i in total xylene (—)
y	Yield (—)
D	Intracrystalline diffusivity (m^2s^{-1})
K	Matrix of dimensionless rate coefficients
L	Characteristic length (m)
T	Temperature (K)
X	Conversion (—)
δ	Depth of penetration of the reaction (m)

Subscripts and Superscripts

m	meta-Xylene
o	*ortho*-Xylene
p	*para*-Xylene
M	Methanol
T	Toluene
X	Xylene
0	At time t = 0
*	At equilibrium

REFERENCES

1. Csicsery, S. M., *in* "Zeolite Chemistry and Catalysis" (J. A. Rabo, Ed.), p. 680. ACS Monograph No. 171, Washington, DC, 1976.
2. Csicsery, S. M., *Zeolites* **4,** 202 (1984).
3. Weisz, P. B., and Frilette, V. J., *J. Phys. Chem.* **64,** 382 (1960).
4. Weisz, P. B., Frilette, V. J., Maatman, R. W., and Mower, E. B., *J. Catal.* **1,** 307 (1962).
5. Chutoransky, P., Jr., and Dwyer, F. G., *in* "Molecular Sieves" (W. M. Meier and J. B. Uytterhoeven, Eds.), p. 540. Advances in Chemistry Series, Vol. 121, Washington, DC, 1973.
6. Chen, N. Y., and Garwood, W. E., *J. Catal.* **52,** 453 (1978).
7. Chen, N. Y., Kaeding, W. W., and Dwyer, F. G., *J. Am. Chem. Soc.* **101,** 6783 (1979).
8. Wei, J., *J. Catal.* **76,** 433 (1982).
9. Kaeding, W. W., Chu, C., Young, L. B., Weinstein, B., and Butter, S. A., *J. Catal.* **67,** 159 (1981).
10. Young, L. B., Butter, S. A., and Kaeding, W. W., *J. Catal.* **76,** 418 (1982).
11. Yashima, T., Sakaguchi, Y., and Namba, S., *in* "Proceedings, 7th International Congress on Catalysis, Tokyo, 1980" (T. Seiyama and K. Tanabe, Eds.), p. 739. Stud. in Surf. Science and Catal., Vol. 7A, Elsevier, Amsterdam, 1981.
12. Bhat, S. G. T., J. Catal. **75,** 196 (1982).
13. Fraenkel, D., Cherniavsky, M., and Levy, M., *in* "Proceedings, 8th International Congress on Catalysis, Berlin, 1984," Vol. IV, p. 545. Verlag Chemie, Weinheim, 1984.
14. Derewinski, M., Haber, J., Ptaszynski, J., Shiralkar, V. P., and Dzwigaj, S., *in* "Structure and Reactivity of Modified Zeolites" (P. A. Jacobs, N. I. Jaeger, P. Jírů, V. B. Kazansky, and G. Schulz-Ekloff, Eds.), p. 209. Stud. in Surf. Science and Catal., Vol. 18, Elsevier, Amsterdam, 1984.
15. Ducarme, V., and Védrine, J. C., *Appl. Catal.* **17,** 175 (1985).
16. Bezouhanova, C., Dimitrov, C., Nenova, V., Spassov, B., and Lechert, H., *Appl. Catal.* **21,** 149 (1986).
17. Ashton, A. G., Batmanian, S., Dwyer, J., Elliott, I. S., and Fitch, F. R., *J. Mol. Catal.* **34,** 73 (1986).
18. Giordano, K., Pino, L., Cavallaro, S., Vitarelli, P., and Rao, B. S., *Zeolites* **7,** 131 (1987).

19. Cavallaro, S., Pino, L., Tsiakaras, P., Giordano, K., and Rao, B. S., *Zeolites* **7,** 408 (1987).
20. Chen, N. Y., *J. Catal.* **114,** 17 (1988).
21. Reschetilowski, W., Siegel, H., and Maschke, B.-H., *Z. Anorg. Allg. Chem.* **573,** 231 (1989).
22. Jahn, S. L., and Cardoso, D., *Catal. Today* **5,** 515 (1989).
23. Fraenkel, D., and Levy, M., *J. Catal.* **118,** 10 (1989).
24. Bauer, F., Dermietzel, J., and Jockisch, W., *in* "Catalysis and Adsorption by Zeolites" (G. Öhlmann, H. Pfeifer, and R. Fricke, Eds.), p. 305. Stud. in Surf. Science and Catal., Vol. 65, Elsevier, Amsterdam, 1991.
25. Prinz, D., and Riekert, L., *Appl. Catal.* **37,** 139 (1988).
26. Beschmann, K., "Der Einfluß von innerkristallinen Transportvorgängen auf die Umsetzung von Methylbenzolen an Zeolithen der MFI-Struktur." Dissertation, Karlsruhe, 1992.
27. Hastings, S. H., and Nicholson, D. E., *J. Chem. Eng. Data* **6,** 1 (1961).
28. Nunan, J., Cronin, J., and Cunningham, J., *J. Catal.* **87,** 77 (1984).
29. Beschmann, K., Kokotailo, G. T., and Riekert, L., *Chem. Eng. Process.* **22,** 223 (1987).
30. Bülow, M., Caro, J., Röhl-Kühn, B., and Zibrowius, B., *in* "Zeolites as Catalysts, Sorbents and Detergent Builders" (H. G. Karge and J. Weitkamp, Eds.), p. 505. Stud. in Surf. Science and Catal., Vol. 46, Elsevier, Amsterdam, 1989.
31. Haag, W. O., *in* "Proc. 6th Int. Zeol. Conf., 1983," p. 466. Butterworths, London, 1984.
32. Qureshi, W. R., and Wei, J., *J. Catal.* **126,** 126 (1990).
33. Tsikoyiannis, J. G., and Wei, J., *Chem. Eng. Sci.* **46,** 255 (1991).
34. Mirth, G., and Lercher, J. A., *J. Catal.* **132,** 244 (1991).